Simulations of Action of DNA Topoisomerases to Investigate Boundaries and Shapes of Spaces of Knots

Alessandro Flammini,*†‡ Amos Maritan,† and Andrzej Stasiak‡
*International School for Advanced Studies, Trieste, Italy; †Department of Physics "G. Galilei" of the University of Padua, Padua, Italy; and ‡Laboratory of Ultrastructural Analysis, Department of Biology and Medicine, University of Lausanne, 1015 Lausanne-Dorigny, Switzerland

ABSTRACT The configuration space available to randomly cyclized polymers is divided into subspaces accessible to individual knot types. A phantom chain utilized in numerical simulations of polymers can explore all subspaces, whereas a real closed chain forming a figure-of-eight knot, for example, is confined to a subspace corresponding to this knot type only. One can conceptually compare the assembly of configuration spaces of various knot types to a complex foam where individual cells delimit the configuration space available to a given knot type. Neighboring cells in the foam harbor knots that can be converted into each other by just one intersegmental passage. Such a segment-segment passage occurring at the level of knotted configurations corresponds to a passage through the interface between neighboring cells in the foamy knot space. Using a DNA topoisomerase-inspired simulation approach we characterize here the effective interface area between neighboring knot spaces as well as the surface–to-volume ratio of individual knot spaces. These results provide a reference system required for better understanding mechanisms of action of various DNA topoisomerases.

INTRODUCTION

A statistical ensemble of long circular polymers in solution like DNA, for example, can reach its highest entropy state only when the circular polymers are permitted to attain the topological equilibrium resulting in the production of a characteristic spectrum of various knots (Dean et al., 1985; Rybenkov et al., 1993; Shaw and Wang, 1993; Deguchi and Tsurusaki, 1994; Katritch et al., 2000). In the case of circular DNA molecules specific enzymes called topoisomerases allow intersegmental passages and therefore may let the molecules reach the topological equilibrium, even if all molecules had the same topology before addition of the enzyme (Krasnow et al., 1983; Dean et al., 1985). Actually, only a subclass of topoisomerases, belonging to the class IA, can bring the system to the topological equilibrium since intersegmental passages mediated by these enzymes are driven by the free energy gradient (Stasiak, 2003), and topoisomerases of type IA can perform knotting and unknotting of single-stranded DNA as well as of double-stranded DNA if the latter contains at least one short interruption in one of the strands (Dean et al., 1985; Champoux, 2001).

In recent years several independent studies investigated how ATP-hydrolysis-driven type II topoisomerases can selectively lower the frequency of DNA knotting (Rybenkov et al., 1997; Yan et al., 1999; Vologodskii et al., 2001). However, there were no systematic studies that investigated the most likely relaxation path of a given DNA knot by a hypothetical topoisomerase that does not show a chirality bias and is just driven by the free energy gradient. Characterization of this relatively simple situation provides a necessary reference required for the understanding of such subtleties of topoisomerase action as the chirality bias (Roca, 2001; Charvin et al., 2003; Stone et al., 2003; Schvartzman and Stasiak, 2004; Trigueros et al., 2004) or differential relaxation of various types of crossings in DNA twist knots (Mann et al., 2004).

We investigate here the case of knotted polymers with 33 statistical Kuhn segments that form freely jointed isolateral polygons with 33 edges. We have selected this size since it corresponds to double-stranded DNA of bacteriophage P4 that provides a convenient experimental system of DNA knotting (Arsuaga et al., 2002a,b). However, our study has a more general perspective, as we aim to investigate generic knot spaces accessible to all polymers that are conveniently modeled as freely jointed, isosegemental chains (Vologodskii et al., 1974; Smith et al., 1992; Deutsch, 1999; Katritch et al., 2000; Arsuaga et al., 2002b; Millett and Rawdon, 2003).

MATERIALS AND METHODS

The evolution of the polygonal chain was achieved via a succession of crank-shaft rotations. Two nonconsecutive vertices of the polygon were selected randomly (with the maximum distance of eight segment units along the chain) and then rotated around the axis passing through the selected vertices. The angle of rotation was drawn with uniform probability between 180° and −180°. The occurrence of intersegmental passages was detected by checking for intersections between the surface of revolution generated by the rotating portion of the chain and segments of the subchain that were not rotated. Our results were of course affected by statistical errors. Statistical

Submitted May 12, 2004, and accepted for publication August 6, 2004.

Address reprint requests to Andrzej Stasiak, Tel.: 41-21-692-42-82; Fax: 41-21-692-41-05; E-mail: andrzej.stasiak@lau.unil.ch.

Alessandro Flammini's present address is School of Informatics, Indiana University, 901 E. 10th St., Bloomington, IN 47408.

0006-3495/04/11/2968/08 $2.00

doi: 10.1529/biophysj.104.045864

fluctuations in our simulations caused, for example, random passages in unknots (0_1) to produce left-handed trefoils (3_{1L}) with a probability of 0.02165 and right-handed trefoils (3_{1R}) with a probability of 0.02395. To compensate for statistical fluctuations and to reestablish the left-right symmetry in our system we averaged over the two data sets, obtaining that the probability of a passage from an unknot to a trefoil knot is of 0.0228, irrespectively of the handedness of the resulting trefoil. Upon imposition of a detailed balance (read below) this value was changed to 0.0227 (see Table 1). The symmetry establishing procedure involved averaging over probabilities of creation of corresponding chiral knots from achiral knots and also averaging over probability of formation of achiral knots and pairs of chiral isoforms from two chiral isoforms of a given knot type. Using the effective rates of strand passage outcomes from individual knot spaces we calculated the expected stationary probabilities of each knot type at the thermodynamic equilibrium. The stationary probabilities values for various knots are the entries of the eigenvector corresponding to the eigenvalue 1 of the transition matrix (Grimmet and Stirzaker, 1992) (see Table 1).

In our simulations each knot type undergoes relaxation independently from other knot types; therefore, it was important to verify whether our method allows us to predict behavior of the system at thermodynamic equilibrium. At thermodynamic equilibrium the number of configurations switching from knot A to B should be equal to those switching from knot

TABLE 1 Probability that a knot type converts into another by a random intersegmental passage

	Starting knot types									
Resulting knot types	0_1	3_{1R} or 3_{1L}	4_1	5_{1R} or 5_{1L}	5_{2R} or 5_{2L}	6_{1R} or 6_{1L}	6_{2R} or 6_{2L}	6_3	$3_{1R}\#3_{1L}$	$3_{1R}\#3_{1R}$ or $3_{1L}\#3_{1L}$
0_1	0.5988 **0.9457** 0.9038	0.6844 0.9276		0.2820 0.3610	0.2669 0.3246	0.1881 0.2281	0.2921 0.3528			
3_{1R} or 3_{1L}	0.0227 0.4180	**0.3374**	0.6534 0.8541	0.4182 0.5353		0.2717 0.3294	0.2679 0.3236	0.4129 0.5000	0.8304 1.0000	
4_1	0.0073 0.1345	**0.2622**			0.4379 0.5325	0.3178 0.3852				
5_{1R} or 5_{1L}	0.0246 0.0372		**0.2350**	0.0811 0.1038						
5_{2R} or 5_{2L}	0.0006 0.0102	0.0217 0.0328	0.1116 0.1459	**0.2187**						
6_{1R} or 6_{1L}	0.0001 0.0016	0.0132 0.0179			0.0508 **0.1775** 0.0618	0.0473 0.0573				
6_{2R} or 6_{2L}	0.0001 0.0016	0.0033 0.0049	0.0136 0.0183		0.0668 0.0812	**0.1750**				
6_3	0.0002 0.0028	0.0036 0.0054					**0.1721**			
$3_{1R}\#3_{1L}$	0.0057 0.0086							**0.1742**		
$3_{1R}\#3_{1R}$ or $3_{1L}\#3_{1L}$	0.0049 0.0074								**0.1696**	

We apply here a modified Alexander-Briggs notation of knots, where the first number indicates the minimal crossing number, the subscript number indicates the tabular position among the knots with the same minimal crossing number (for the tables see Rolfsen, 1976; Adams, 1994) and the subscripts $_R$ or $_L$ indicate right- or left-handed form of a given knot. The analyzed knots include three achiral prime knots (0_1, 4_1, and 6_3), five pairs of chiral prime knots (3_1, 5_1, 5_2, 6_1, 6_2) in their right- and left-handed form, and three composite knots composed of two trefoils in three possible combinations ($3_{1R}\#3_{1R}$, $3_{1L}\#3_{1L}$, and $3_{1R}\#3_{1L}$). The starting configurations are indicated in the upper row whereas resulting knots are marked in the left column. The entries correspond to the probability with which knots listed in the upper panel gets converted into knots listed in the left panel (but not the contrary). Upper and middle entries (*in bold*) in the relevant rows indicate the probability with which a given knot can change to another knot or remain the same, respectively. The sum in every column over upper and middle entries taken together is 1 for all chiral starting knots. For achiral starting knots the upper entries indicating passages to chiral knots need to be counted twice since the listed entries indicate probabilities of passages to each of enantioforms of chiral knots. Notice that the data in the table have been corrected to reestablish left-right symmetry and brought to the detailed balance situation (see Methods). The lower entries in respective rows indicate the probabilities of exiting a given knot space to other spaces when only passages that resulted in a change of the knot type were considered.

B to A. For example the stationary probability of unknots multiplied by the transition rate from unknots to right-handed trefoils should be equal to the stationary probability of right-handed trefoils multiplied by the transition rate from right-handed trefoils to unknots. In our case the respective products amounted to 0.0208 and 0.0206. The observed deviations from the detailed balance condition were also very small for other pairs of knots and probably resulted only from statistical fluctuations. We therefore imposed the detailed balance into the data presented in Table 1 in such a way that the stationary probability of every knot type remained unchanged.

RESULTS

One passage connectivity between neighboring knot spaces

Our investigation of knot spaces is based on simulations of an experiment in which highly diluted polymer molecules, forming various knot types, undergo random intersegmental passages and where, after each intramolecular segment-segment passage, the topology of the molecules is determined. To obtain a random configuration of a given knot type we start with a polygonal configuration that resembles the axial trajectory of so-called ideal knots of a given type (Katritch et al., 1996; Buck, 1998; Stasiak et al., 1998). These starting configurations are then evolved as nonphantom chains by applying random crank-shaft moves (Vologodskii et al., 1992). Nonphantom evolution is achieved by accepting only these crank-shaft moves during which there are no segment-segment passages. After 20,000 of such accepted random moves, when the configuration is sufficiently randomized, the polygon is further evolved by random crank-shaft rotations but in addition moves that result in just one intersegmental passage are also accepted. After the first passage the evolution is terminated and the knot type of the polygonal chain is determined by calculation of its HOMFLY polynomial (Freyd et al., 1985; Ewing and Millett, 1996; Dobay et al., 2003). The entire procedure was repeated 20,000 times for each analyzed knot type. We investigated what happens after a passage to all types of knots with up to six crossings, whereas passages leading to formation of knots with seven or more crossings were not entered into the statistics.

Table 1 lists the probabilities with which a random passage in a given knot type (the starting knot types are indicated in the head of the table) leads to emergence of a new trajectory of the same or a different knot type (the types of resulting knots are indicated on the left side of the table). There are three sorts of data in the Table 1. Upper entries in corresponding cells are the transition probabilities with which a given starting knot can change its knot type to the respective resulting knots in an experiment in which passages resulting in no change of original topology are also taken into account. The middle entries (*underlined*) in diagonal fields of the table list probabilities that a given knot does not change its knot type after one segment-segment passage. The lower entries in respective cells result from a renormalization of the data by taking into account only these passages that have led to the change of the knot type. Looking at Table 1 one can see, for example, that random intersegmental passages in unknots (*first column*) led in almost 95% of cases back to the same knot type (*underlined*). Fig. 1 *a* presents an example of such a passage that does not change the knot type. Table 1 also shows that if only the passages that resulted in a change of the knot type were analyzed (lower entries), then right- and left-handed trefoil knots were both produced with almost 42% efficiency from unknots (see Methods section for the information how left-right symmetry was obtained from the data). Figure-of-eight knots, that are achiral, were produced in ~13% of knot type-changing passages from unknots, whereas 5_{2R} and 5_{2L} knots were both produced with ~1% probability. More complex knots emerged from unknots with still lower probabilities.

It is also visible that 5_1 knots did not arise from unknots by one strand passage. This reflects the fact that at least two

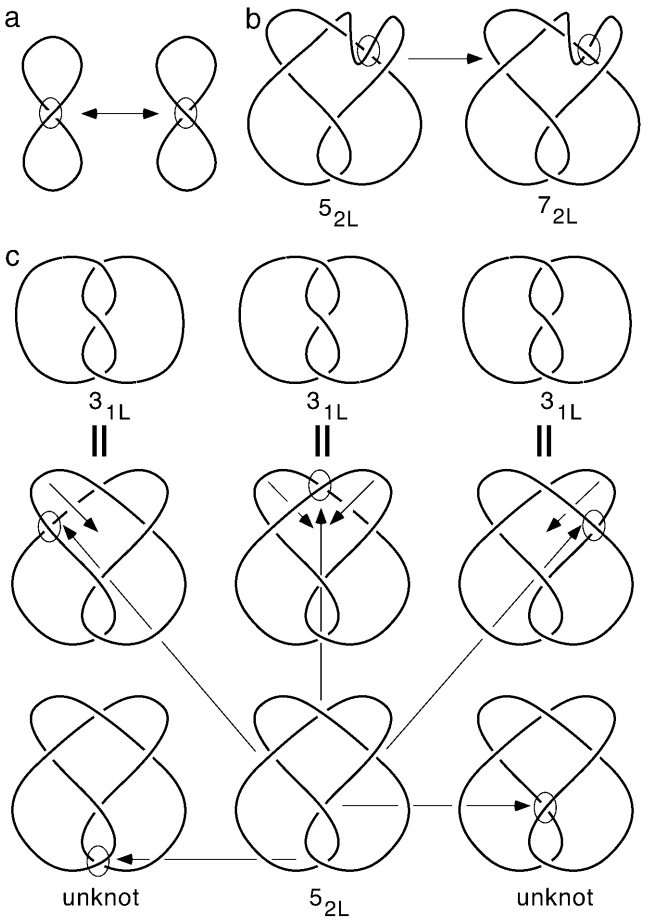

FIGURE 1 Effects of intramolecular segment-segment passages. (*a*) Example of a passage that does not change the topology of analyzed trajectory. (*b*) To create more complex knots out of simpler knots, the latter need to show some additional, nonessential crossings where segment-segment passage could occur. (*c*) Segment-segment passages acting on minimal crossing representation of a 5_2 knot create in three out of five cases trefoil knots and in the remaining cases unknots. Thin ellipses denote sites of segment-segment passages.

strand passages are required to pass from an unknot to 5_1 knot (Darcy and Sumners, 1997, 2000). The same applies to the passage from a 3_1 to 4_1 knot (and vice versa). One can also see (*column 5*) that configurations forming knot 5_2 exit more frequently to space of 3_1 knots than to space of unknots. This result can be intuitively expected since out of five possible passages performed at the crossing points of standard, minimal crossing representation of 5_2 knot, three passages lead to formation of trefoils (3_1 knots) whereas two passages lead to formation of unknots (0_1 knots) (Fig. 1 *c*). Of course, minimal crossing representations do not reflect all possible random configurations of a given knot and do not explain, for example, how 5_2 knot can be converted by one passage to 5_1 knot or to higher knots. Configurations with additional, nonessential crossings are required to permit these types of passages (see Fig. 1 *b*).

The observed one-passage connections within knots with up to six crossings agree with earlier analytical treatment of this subject (Darcy and Sumners, 1997, 2000). We observed transitions between all these knot spaces that are separated by one passage and didn't observe any when more than one passage is needed for such a change (Darcy and Sumners, 1997, 2000). We believe, therefore, that our simulation procedure probes adequately the connectivity between different knot spaces. Our studies go however further than revealing one-passage connectivity between different knot spaces since we obtain quantitative information about the extent of contact between the neighboring knot spaces.

Interfaces and shapes of individual knot spaces

By monitoring ratios of probabilities with which random configurations of studied knots exit by random passages to different neighboring knot spaces we can probe the effective interface area between corresponding knot spaces. The effective interface areas between different knot spaces are defined operationally as proportional to the number of observed passages between the knots in question. However, if different interfaces vary in their curvature and corrugation, then the actual interface areas may not be proportional to the corresponding effective interface areas. The lower entries in corresponding cells in Table 1 reflect the relative effective interface area of individual knot spaces with other knot spaces. Notice that the global interface of the starting knot space with all neighboring spaces is normalized to one for every individual knot type (sum of lower entries in every column is 1, taking into account that there are always two different chiral knots of the corresponding type). One can see, for example, that $>41\%$ of the surface enclosing the space of unknots forms an interface with the space of right-handed trefoils (*first column, second row* in Table 1). On the other side, $>90\%$ of the surface enclosing the configuration space occupied by right-handed trefoils is shared with the surface that encloses unknots (*second column, first row*). It should be obvious that the interface of the space of unknots with the space of right-handed trefoils has to be equal to the interface of the space of right-handed trefoils with the space of unknots. Therefore, one can simply conclude that the total surface enclosing the space of unknots is $\sim$2.16 times bigger than the corresponding surface enclosing right-handed trefoils.

The same type of calculation can be performed for any pair of knots with one-passage connectivity. Using this method we can express the delimiting surface of various knot spaces as a fraction of the total surface of all knot spaces summed together and taken as 1. For 33-segments long freely jointed polygons the knots 0_1, 3_{1R} or 3_{1L}, 4_1, 5_{1R} or 5_{1L}, 5_{2R} or 5_{2L}, 6_{1R} or 6_{1L}, 6_{2R} or 6_{2L}, 6_3, $3_{1R}\#3_{1R}$ or $3_{1L}\#3_{1L}$, and $3_{1R}\#3_{1L}$ have the following delimiting surfaces: 0.4518, 0.2090, 0.0655, 0.0091, 0.0128, 0.0022, 0.0031, 0.0035, 0.0015, and 0.0036, respectively, with a $\sim$10% error.

Diagonal entries in Table 1 (*underlined*) tell us how frequently configurations representing a given knot type remain in the same knot space after a random strand passage. It is visible that, as the knots get more complex their tendency to remain in the same knot type decreases. The probability of remaining in the same knot space after a random passage reflects the ratio between the area of internal invaginations (passage through which does not change the knot type) and the area of the external surfaces which separate different knot types. If the density of internal invaginations in various knot spaces is similar, the probability of remaining in the same knot space after a random passage reflects in an indirect way the volume-to-surface ratio of individual knot spaces. Thus, for example, a space of unknots seems to have the highest volume to surface ratio, whereas each of the spaces of various six-crossing knots has a much smaller volume-to-surface ratio (Table 1).

It was shown earlier that the so-called ideal geometric representations of knots decrease their volume-to-surface ratios with increasing complexity of knots (Katritch et al., 1996). More recently it was proposed that the relative probability of occurrence of various knots at topological equilibrium should decrease exponentially with the length/diameter ratio (L/D) of their corresponding ideal geometric representations (Grosberg, 1998).

The underlying hypothesis was that the diameter of tubes formed by ideal knots approximates the 3-D space available to a given knot type (Grosberg et al., 1996; Grosberg, 1998) and that this, in turn, is directly correlated to the probability of occurrence of the knot, or, in other words, to the volume of the high-dimensional configuration space available to that knot type.

This proposal, however, failed to explain why the probability of occurrence of 5_2 knots is significantly higher than that of 5_1 knots, despite the fact that 5_2 knots show higher L/D ratio of their ideal configurations (Deguchi and Tsurusaki, 1994; Katritch et al., 1996).

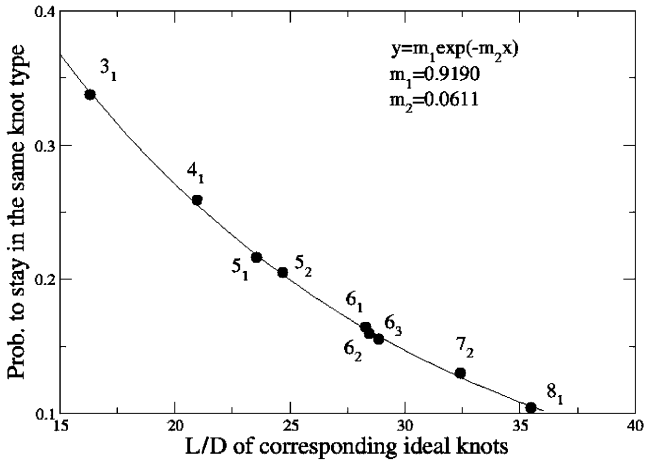

FIGURE 2 Probability of remaining in the same knot type upon one random segment-segment passage decreases exponentially with the L/D of corresponding ideal knots. (L/D values of ideal knots are taken from Katritch et al., 1996). The data points included knots 7_2 and 8_1 as we wanted to extend the range of analyzed knots to higher L/D values. The probability values of remaining in the same knot type plotted in this figure are slightly different from those listed in the Table 1 as we did not limit our statistics here to the passages that do not create knots with more than six crossings.

The core of the issue is, therefore, whether there is a relation between the physical 3-D space available for configurations of a given knot and the high dimensional configuration space occupied by the same knot type.

In the studied system the equilibrium probability of occurrence of a given knot type (volume of the high-dimensional configuration space) is the result of the complex dynamical process that, via intersegmental passages, allow the chain to maintain or change its knot type with different probabilities. The probability to stay in a given knot type after a pivotal type of move depends, however, on the extent of the 3-D space within which the configuration can move without self intersections leading to the change of the knot type. We suggest, therefore, that only the probability to maintain the knot topology is directly related to L/D ratio of ideal representations of knot. Fig. 2 shows that the probability of remaining in the same knot type upon a random segment-segment passage exhibits in fact an exponential decrease with L/D ratio of ideal knots and is consistent with the fact that 5_1 knots, despite their lower probability of formation, are more ''stable'' than 5_2 knots.

To conclude, L/D ratio of an ideal knot only partially accounts for the equilibrium probability of the given knot. Equilibrium properties, in fact, can be effectively sampled only if the full connectivity of high-dimensional configuration space is considered.

Intensity of exchanges between all investigated knot spaces

Fig. 3 illustrates the connectivity diagram of the analyzed knot types together with their expected probability. Fig. 3 presents only achiral knots and right-handed isoforms of chiral knots. Left-handed isoforms would be placed symmetrically on the left side of the ''reflecting plane'' occupied by achiral knots 0_1, 4_1, 6_3, and $3_{1R}\#3_{1L}$. Fig. 3 allows us to quickly find the minimal number of passages required for passing from one knot type to another. For example, to pass from the space of 5_{1R} knots to that of unknots, two passages are needed and two more would be needed to reach the space of 5_{1L} knots. In Fig. 3 we also indicated the intensity of exchanges or fluxes between neighboring knot spaces at thermodynamic equilibrium. The fluxes resulting from random passages between neighboring knot spaces are normalized with respect to the flux between unknots and each of trefoil-knots (the intensity of which was taken as 1).

Map of knot spaces

One is tempted to sketch a map of knot spaces. Of course knot spaces are of higher dimensions but one can imagine a conceptual flattening of these spaces into a planar map as in Fig. 4. We have tried to keep the relative order of surfaces of individual knot territories corresponding to the observed order of their probability. Right- and left-handed enantioforms were placed on the right- and left-side, respectively, with a distance from the vertical axis roughly proportional to the mean writhe of the corresponding random knots (Le Bret, 1980; Katritch et al., 1996; Janse Van Rensburg et al., 1998). Achiral knots are, therefore, centered along the vertical axis. We also tried to put more complex knots ''higher'' than simpler knots.

Our map presents just one of many possible arrangements that satisfy the established connectivity between different knot spaces (presented as overlapping patches). Note that 6_{1R} and 6_{1L} knots are neighbors in the configuration space (this was not visible in Fig. 3). The map applies to the random polygon composed of 33 freely jointed segments we studied here and it would change with the size of the chain. In case of much longer chains knots will dominate over unknots and every individual knot type will be very rare but there will be many different knots. Despite this chain-size dependence of the map, the knots that are neighbors in the case of 33 segments long chains will remain neighbors also for very long chains. It should be clear, however, that the shown map is only a conceptual aid in understanding complex connectivity in multidimensional knot spaces.

Knot spaces are usually sampled using a phantom chain evolution; however, such a sampling can only provide information about expected stationary probabilities of different knots without revealing the overall organization of the entire knot space (Rybenkov et al., 1993; Deguchi and Tsurusaki, 1994; Katritch et al., 2000). It is important to mention though, that the expected stationary probabilities obtained with phantom sampling closely coincided with these obtained from nonphantom exploration (data not

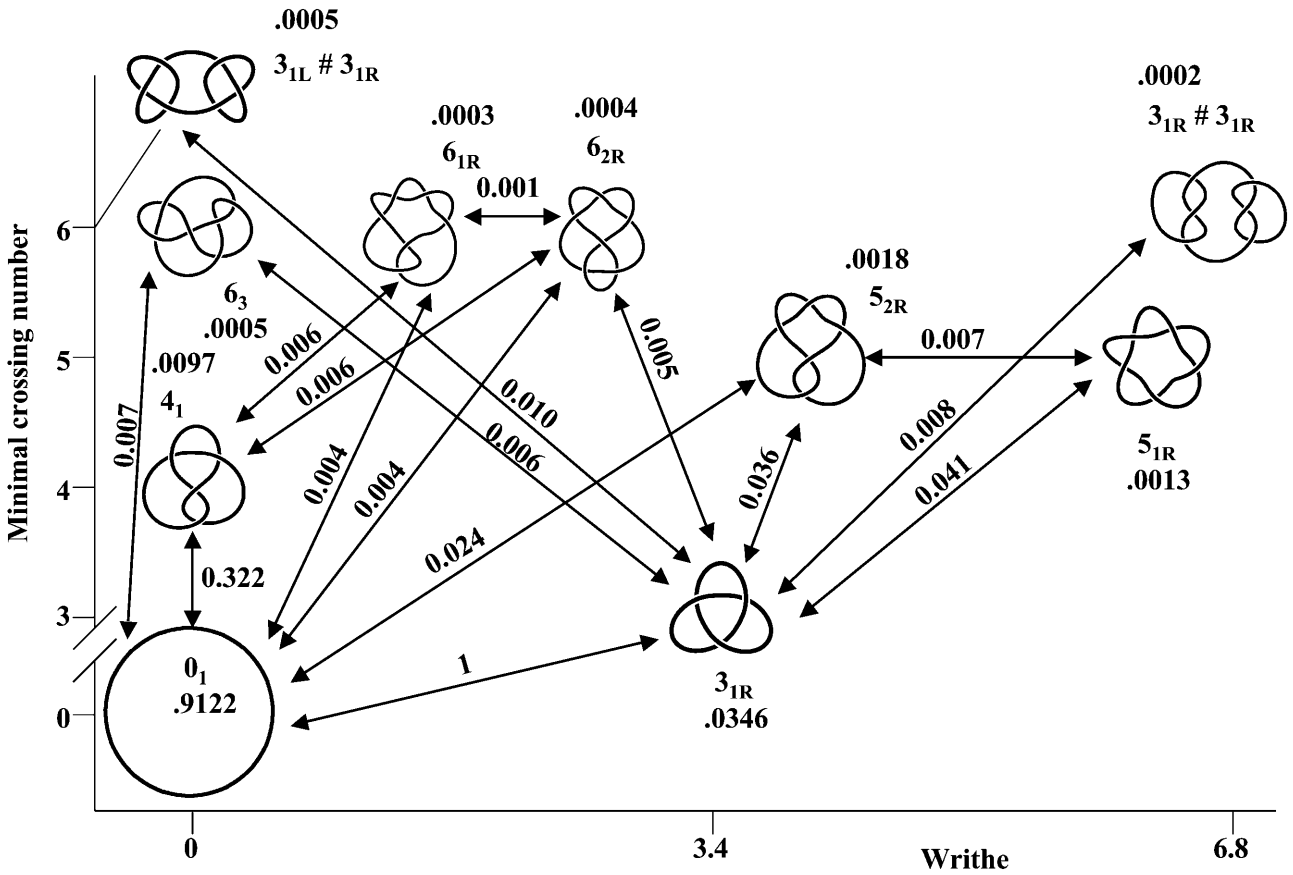

FIGURE 3 One-passage connectivity diagram of knots with up to six crossings. The diagram presents achiral knots and right-handed enantiomorphs of chiral knots. Left-handed enantiomorphs would be positioned symmetrically, with the corresponding negative values of writhe. The knots are arranged according to their writhe values that is a measure of chirality and according to their minimal crossing number. Stationary probabilities, calculated using the data in Table 1, are indicated for each knot type. The intensities of fluxes between neighboring knot spaces are expressed as a fraction of exchanges between unknots and 3_{1R} of 3_{1L} knots. Not all digits are significant. We estimate the error range at ~10% on the basis of performing the calculation with twice smaller data set. Notice that the numerical values in the diagram will change for longer chain sizes, however, the connectivity will remain the same.

shown) indicating that the structure of the foamy knot space is not affected by the particular polymer dynamics applied in our simulation studies.

Using the topoisomerase-inspired approach presented here, we were able to verify earlier theoretical studies that investigated which knots are neighbors in the knots configuration space (Darcy and Sumners, 1997, 2000). In addition, we were able to characterize the extent of contacts, and thus exchanges, between configuration spaces of different knots. The probabilities of staying in the same knot type after a random passage provided us with an estimation of the surface-to-volume ratio of configuration spaces of various knots.

Biological applications

The presented methodology can be applied to quantify biases manifested by some DNA topoisomerases during relaxation of particular types of DNA knots. It was reported recently that type II topoisomerases act preferentially on clasp crossings in twist 5_2 knots (Mann et al., 2004). However, the actual extent of the bias can be only quantified when one knows what the probability of acting on the clasp crossing in the absence of any bias is. Table I shows that without any bias the action on the clasp crossing on 5_2 knot tied on 10-kb-long DNA should happen in ~36% of strand passages that result in the change of the knot type. Therefore, if the probability of action of the investigated topoisomerase II on the clasp crossing is significantly >36% the bias can be confirmed.

Another example where the probabilities of passages between different knot types can be used to obtain biologically significant information concerns the geometry of DNA packing inside phage heads. The DNA knots formed within phage heads can provide hints about the nature of DNA packing (Arsuaga et al., 2002b) but the knots are too complex for their knot type to be determined by electron-microscopy (Krasnow et al., 1983) or by their electrophoretic migration (Vologodskii et al., 1998). However, upon partial relaxation knots become simpler and can be correctly

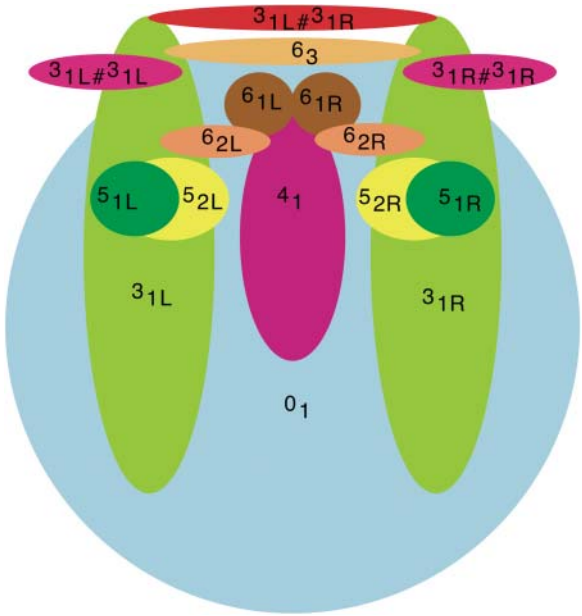

FIGURE 4 Schematic ''flattened'' map of knot spaces of all knots with up to six crossings. Achiral knots are centered along the vertical axis, whereas chiral enantioforms are placed on the right- or left-hand side of the vertical axis.

recognized by their electrophoretic migration (Arsuaga et al., 2002b). The methodology presented here should allow finding out what were the knots that produced the partially relaxed knots of a known knot type. The probability of a passage from one knot to another as a result of individual topoisomerase reactions can not be obtained from the classical exploration of the knot space where the equilibrium probabilities of different knots are calculated (Rybenkov et al., 1993).

We thank G. Buck, P. De Los Rios, A. Dobay, J. Dubochet, and K. Millett for valuable discussions.

This research was funded in part by Swiss National Science Foundation grants 3152-068151 and 3100A0-103962.

REFERENCES

Adams, C. C. 1994. The Knot Book. W. H. Freeman and Company, New York.

Arsuaga, J., R. K. Tan, M. Vazquez, D. W. Sumners, and S. C. Harvey. 2002a. Investigation of viral DNA packaging using molecular mechanics models. *Biophys. Chem.* 101–102:475–484.

Arsuaga, J., M. Vazquez, S. Trigueros, D. W. Sumners, and J. Roca. 2002b. Knotting probability of DNA molecules confined in restricted volumes: DNA knotting in phage capsids. *Proc. Natl. Acad. Sci. USA.* 99:5373–5377.

Buck, G. 1998. Four-thirds power law for knots and links. *Nature.* 392:238–239.

Champoux, J. J. 2001. DNA topoisomerases: structure, function, and mechanism. *Annu. Rev. Biochem.* 70:369–413.

Charvin, G., D. Bensimon, and V. Croquette. 2003. Single-molecule study of DNA unlinking by eukaryotic and prokaryotic type-II topoisomerases. *Proc. Natl. Acad. Sci. USA.* 100:9820–9825.

Darcy, I. K., and D. W. Sumners. 1997. A strand passage metric for topoisomerase action. *In* Knots '96: Proceedings of the Fifth MSJ International Research Institute of Mathematical Society of Japan. S. Suzuki, editor. World Scientific, Singapore.

Darcy, I. K., and D. W. Sumners. 2000. Rational tangle distance on knots and links. *Math. Proc. Cambridge Philos. Soc.* 128:497–510.

Dean, F. B., A. Stasiak, T. Koller, and N. R. Cozzarelli. 1985. Duplex DNA knots produced by *Escherichia coli* topoisomerase I, structure and requirements for formation. *J. Biol. Chem.* 260:4975–4983.

Deguchi, T., and K. Tsurusaki. 1994. A statistical study of random knotting using the Vassiliev invariants. *Journal of Knot Theory and Its Ramifications.* 3:321–353.

Deutsch, J. M. 1999. Equilibrium size of large ring molecules. *Phys. Rev. E.* 59:R2539–R2541.

Dobay, A., J. Dubochet, K. Millett, P.-E. Sottas, and A. Stasiak. 2003. Scaling behavior of random knots. *Proc. Natl. Acad. Sci. USA.* 100:5611–5615.

Ewing, B., and K. C. Millett. 1996. Computational algorithms and the complexity of link polynomials. *In* Progress in Knot Theory and Related Topics, Trauaux en Cours. 56. Hermann. Paris. 51–68.

Freyd, P., D. Yetter, J. Hoste, W. Lickorish, K. Millett, and A. Ocneau. 1985. A new polynomial invariant of knots and links. 12:239–246.

Grimmet, G., and D. Stirzaker. 1992. Probability and Random Processes. Oxford University Press, Oxford.

Grosberg, A. Y. 1998. Entropy of a knot: simple arguments about difficult problem. *In* Ideal Knots. A. Stasiak, S. Katritch, and L. H. Kauffman, editors. World Scientific, Singapore. 129–142.

Grosberg, A. Y., A. Feigel, and A. Rabin. 1996. Flory-type theory of a knotted ring polymer. *Phys. Rev. E.* 54:6618–6622.

Janse Van Rensburg, E. J., D. W. Sumners, and S. G. Whittington. 1998. The writhe of knots and links. *In* Ideal Knots. A. Stasiak, S. Katritch, and L. H. Kauffman, editors. World Scientific, Singapore. 70–87.

Katritch, V., J. Bednar, D. Michoud, R. G. Scharein, J. Dubochet, and A. Stasiak. 1996. Geometry and physics of knots. *Nature.* 384:142–145.

Katritch, V., W. K. Olson, A. V. Vologodskii, J. Dubochet, and A. Stasiak. 2000. Tightness of random knotting. *Phys. Rev. E.* 61:5545–5549.

Krasnow, M. A., A. Stasiak, S. J. Spengler, F. Dean, T. Koller, and N. R. Cozzarelli. 1983. Determination of the absolute handedness of knots and catenanes of DNA. *Nature.* 304:559–560.

Le Bret, M. 1980. Monte Carlo computation of the supercoiling energy, the sedimentation constant and the radius of gyration of unknotted and knotted circular DNA. *Biopolymers.* 19:619–637.

Mann, J. K., R. W. Deibler, D. W. Sumners, and E. L. Zechiedrich. 2004. Unknotting by type II topoisomerases. Abstracts of papers presented to the American Mathematical Society. 25:994–92–187.

Millett, K. C., and E. J. Rawdon. 2003. Energy, rope length, and other physical aspects of equilateral knots. *J. Comp. Phys.* 186:426–456.

Roca, J. 2001. Varying levels of positive and negative supercoiling differently affect the efficiency with which topoisomerase II catenates and decatenates DNA1. *J. Mol. Biol.* 305:441–450.

Rolfsen, D. 1976. Knots and Links. Publish or Perish Books, Berkeley, CA.

Rybenkov, V. V., N. R. Cozzarelli, and A. V. Vologodskii. 1993. The probability of DNA knotting and the effective diameter of the DNA double helix. *Proc. Natl. Acad. Sci. USA.* 90:5307–5311.

Rybenkov, V. V., C. Ulsperger, A. V. Vologodskii, and N. R. Cozzarelli. 1997. Simplification of DNA topology below equilibrium values by type II topoisomerases. *Science.* 277:690–693.

Schvartzman, J. B., and A. Stasiak. 2004. A topological view of the replicon. *EMBO Rep.* 5:256–261.

Shaw, S. Y., and J. C. Wang. 1993. Knotted DNA rings: probability of formation and resolution of the two chiral trefoils. *Science.* 260:533–536.

Smith, S. B., L. Finzi, and C. Bustamante. 1992. Direct mechanical measurements of the elasticity of single DNA molecules by using magnetic beads. *Science*. 258:1122–1126.

Stasiak, A. 2003. Topoisomerases. *In* Encyclopedia of the Human Genome. Nature Publishing Group, London.

Stasiak, A., J. Dubochet, V. Katritch, and P. Pieranski. 1998. Ideal knots and their relation to the physics of real knots. *In* Ideal Knots. A. Stasiak, S. Katritch, and L. H. Kauffman, editors. World Scientific, Singapore. 1–19.

Stone, M. D., Z. Bryant, N. J. Crisona, S. B. Smith, A. Vologodskii, C. Bustamante, and N. R. Cozzarelli. 2003. Chirality sensing by *Escherichia coli* topoisomerase IV and the mechanism of type II topoisomerases. *Proc. Natl. Acad. Sci. USA*. 100:8654–8659.

Trigueros, S., J. Salceda, I. Bermudez, X. Fernandez, and J. Roca. 2004. Asymmetric removal of supercoils suggests how topoisomerase II simplifies DNA topology. *J. Mol. Biol*. 335:723–731.

Vologodskii, A. V., N. J. Crisona, B. Laurie, P. Pieranski, V. Katritch, J. Dubochet, and A. Stasiak. 1998. Sedimentation and electrophoretic migration of DNA knots and catenanes. *J. Mol. Biol*. 278:1–3.

Vologodskii, A. V., S. D. Levene, K. V. Klenin, M. Frank-Kamenetskii, and N. R. Cozzarelli. 1992. Conformational and thermodynamic properties of supercoiled DNA. *J. Mol. Biol*. 227:1224–1243.

Vologodskii, A. V., A. V. Lukashin, M. D. Frank-Kamenetskii, and V. V. Anshelevitch. 1974. The knot problem in statistical mechanics of polymer chains. *Sov. Phys. JETP* (Engl. Transl.). 39:1059–1063.

Vologodskii, A. V., W. Zhang, V. V. Rybenkov, A. A. Podtelezhnikov, D. Subramanian, J. D. Griffith, and N. R. Cozzarelli. 2001. Mechanism of topology simplification by type II DNA topoisomerases. *Proc. Natl. Acad. Sci. USA*. 98:3045–3049.

Yan, J., M. O. Magnasco, and J. F. Marko. 1999. A kinetic proofreading mechanism for disentanglement of DNA by topoisomerases. *Nature*. 401:932–935.